ISSN 0036-0236, Russian Journal of Inorganic Chemistry, 2024. © Pleiades Publishing, Ltd., 2024.

COORDINATION COMPOUNDS

A Novel Multichromic Cd(II) Coordination Polymer Based on a Viologen Ligand Exhibiting Multichroism, Aniline Detection and Luminescence Properties

Ran Tao[a], Xiuyan Wang[b], Xin Wang[a], Zirui Huang[c], Shanshan Jin[a, *], and Hongqiang Wang[a]

[a] *College of Science, Beihua University, 3999 Binjiang East Road, Jilin, 132013 PR China*

[b] *College of Materials and Textile Engineering, Nanotechnology Research Institute, Jiaxing University, Jiaxing, Zhejiang, 314001 PR China*

[c] *State Key Laboratory of Inorganic Synthesis and Preparative Chemistry, Jilin University, Changchun, 130000 PR China*

**e-mail: bhjss1990@163.com*

Received April 5, 2024; revised June 7, 2024; accepted June 7, 2024

Abstract—As a powerful strategy to precisely fabricate multifunctional materials with unique optoelectronic properties, donor-acceptor (D–A) alignment, which integrates D–A pairs into the modular and versatile crystalline cation metal–organic frameworks (CMOFs) and cation coordination polymers (CCPs) is applied at the molecular level. In this paper, a photo- and thermochromic CCP, named [Cd $(PTA)_{0.5}(bcbpy)_{0.5}Br$] (**1**), was successfully produced by the self-assembly of a photo- and thermoactive 1,1'-bis((3-carboxylatobenzyl)-4,4'-bipyridinium)-dibromo ligand ($H_2bcbpy{\cdot}2Br$) with cadmium chloride and terephthalic acid (PTA). This complex is characterized by single-crystal X-ray diffraction, powder X-ray diffraction and it exhibits high sensitivity to both heat and different illuminant. The exceptional difunctional characteristics of electron-transfer (ET) thermochromism and photochromism in **1** are mostly influenced by the photosensitivity and thermal sensitivity of $H_2bcbpy{\cdot}2Br$. Otherwise, during the coloration-decoloration phase, there is a photoluminescence "on/off switch" which would direct the synthesis of new crystals.

Keywords: viologen, chromic, luminescence properties

DOI: 10.1134/S0036023624601119

INTRODUCTION

Cation coordination polymers (CCPs) and cation metal-organic frameworks (CMOFs), which exhibit color-changing, are the most primary and available materials. Because their demands are increased in luminescence, chromic materials, proton conduction, and sensors, which have attracted tremendous attention [1–7]. Three-dimensional multichromic CCPs and CMOFs are an interesting class of porous sensing materials established from metal center coordinated with functional organic linkers. They have been synthesized by more and more researchers owing to their novel, outstanding compositional structural and functional diversity. Chromic materials have a good response to heat, light, X-rays, electricity, as well as other stimulate, which get wide attention, and have high application potential in organic photovoltaic, thermoelectric generators or light-emitting diodes [8–11]. Color-changing organic-inorganic hybrid materials are a kind of ground-breaking materials and have attracted much attention due to their possible application prospects [12]. Various chromic CCPs and CMOFs named after the stimulate, for example, thermochromic, photochromic, electrochromic, hydrochromism, etc. Furthermore, an interesting feature of this class of chromic materials is the discoloration step, which is the transfer of electrons from the electron donor (d) to electron acceptor (ET) resulted in the generation of free radicals [13–17]. In the development of chromic organic–inorganic hybrids materials, the optical properties of organic ligands are an important strategy for designing materials with multichromic and mumtifunctional applications [14, 15]. Many families of organic and inorganic multichromic materials have been discovered. Among them, the selection of organic species, which objects as the major development for the function of the materials [18–20].

Several chromic organic ligands (piperazine, divinene, naphthalenediimide and violone) have been studied in response to diverse external stimuli [10, 11]. Viologens/bipyridine derivatives (1,1'-disubstituted 4,4'-bipyridine) are widely used as herbicides in a different kind of drugs and medicines, have a long history of research and development, and are famous for their unique electron-lacking properties: one is to form charge transfer complexes with electron-rich sub-

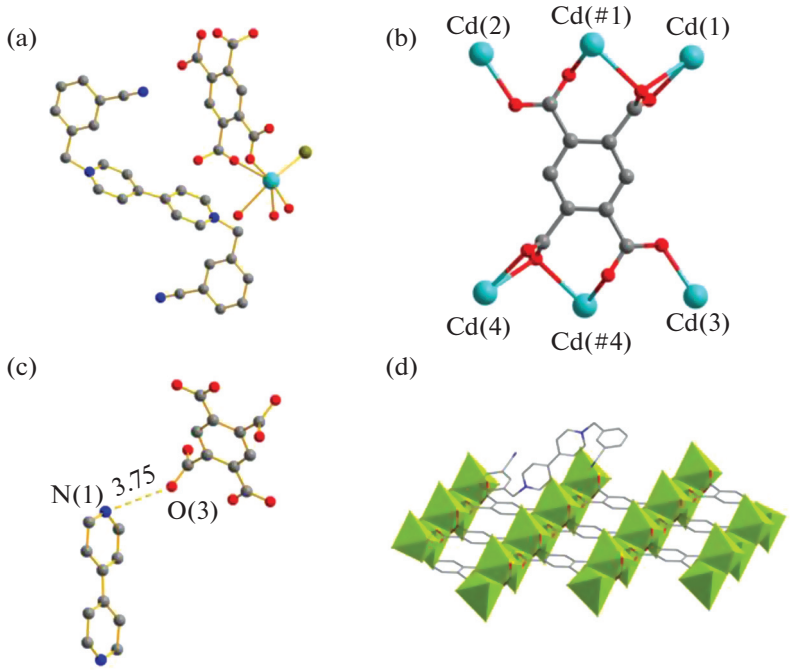

Fig. 1. (a) Coordinated environment in **1**; (b) coordinated environment around PTA4-ligand in **1**; (c) electron transfer approaches of **1**, (d) the packing framework of **1**.

stances (such as organic amines), and the other is to implement reversible electron transfer when were exposed to different kinds of stimuli. The electron-deficient viologen cations (V^{2+}) can form vioiogen radicals ($V^{\cdot}$) by single electron transfer from the suitable electron donor and are always with recognizable colour changing. To construct chromic viologen-based CCPs with the electron transfer (ET) progress, some key factors should be considered, such as the packing type, the distance and orientation between D and A, the hydrogen bonds and so on. But the design and choice of the viologen is the most important.

In this paper, the novel multichromic cation coordination polymer $[Cd(BTC)_{0.5}(bcbpy)_{0.5}Br]$ (**1**) was synthesized from 1,1'-bis (3-cyanobenzene)-[4,4'-bipyridine]-1,1'-dibromide, $CdBr_2{\cdot}4H_2O$ and H_4PTA as raw materials. Compound **1** has great photosensitive activity and is responsive to Uv light and blue light at room temperature. Compound **1** changes color under 365 nm UV light and 405 nm blue light. At the same time, compound **1** is thermochromic when heated at 90°C. The detection and recognition ability of aniline was demonstrated. Uv/vis diffuse reflectance spectra, electron spin resonance (ESR) and theoretucal study were used to increase available and viewpoints about the mechanisms of color rendering progression.

EXPERIMENTAL

All materials were bough commercially and there is no further purification. The viologen synthesis and instrument testing are in the supporting information. The synthetic route and ^1H NMR spectrum of $H_2bcbpy{\cdot}2Br$ (600 MHz, D_2O) are in Figs. S1 and S2.

Synthesis of $[Cd(PTA)_{0.5}(bcbpy)_{0.5}Br]$ (1). With $CdBr_2{\cdot}4H_2O$ (29 mg, 0.1 mmol), pyromellitic acid (25.4 mg, 0.1 mmol), $H_2bcbpy{\cdot}2Br$ (54 mg, 0.1 mmol), DMF (2 mL) and distilled water (3 mL) was thermoscopically reacted to get the light white monocrystalline acicular framework of complex **1**. The mixture was sealed in a 25 mL polytetrafluoroethylene reactor and heated at 90°C for 96 h. Next, the autoclave cooled slowly to indoor temperature. The crystals are gathered via filtration, cleaned with deionized water, subsequently, dried in air. Based on $CdBr_2{\cdot}4H_2O$, the yield of violet ligand was 62% of $C_{18}H_{11}O_4N_2BrCd$. FT-IR (KBr, cm^{-1}): 3300–3500 m, 2260–2215sh, 1642vs, 1586vs, 1541vs, 1481vs, 1367vs, 1250–1140s, 816s, 578s. TGA curve (Fig. S3) shows that in the temperature before ca. 330°C, **1** exhibits a weight loss, this illustrated thatthere were no water and solvent DMF molecules in the framework, which was exactly the structure shown in Fig. 1 and the framework collapses at temperatures from ca. 330 to 700°C.

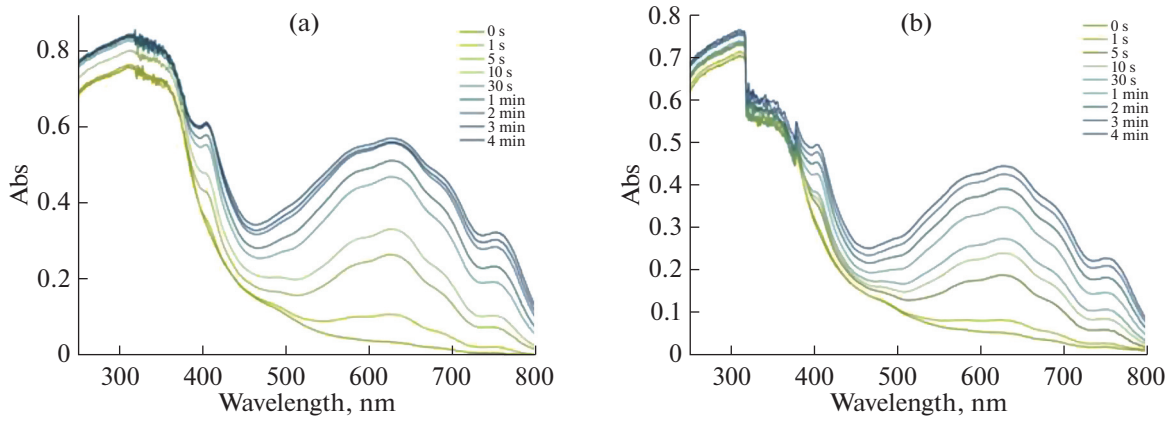

Fig. 2. UV/vis diffuse-reflectance spectral changes to **1** under 365 nm UV light and 405 nm blue light irradiation.

RESULTS AND DISCUSSION

*Crystal Structure of [Cd (PTA)$_{0.5}$(bcbpy)$_{0.5}$Br] (**1**)*

Single-crystal X-ray diffraction (XRD) analysis shows compound **1** crystallized in the triclinic system and its spatial group is *P*-1. Although this class crystals based on the host-guest cluster interaction has been widely reported, this 1D coordination frameworks with the ligand H_2bcbpy·2Br extremely rare. The light-yellow crystal of **1** was obtained by unique design by the counter Br^- viologen ligand and $CdBr_2·4H_2O$, which achieved the coordination of Br^-(Fig. 1). In Fig. 1a, the structure of coordination environment of **1**, the metal Cd coordinated with PTA^{4-} ligand and formed 1D structure. The asymmetric unit was shown in Fig. S4, **1** have anionic framework $[Cd(PTA)_{0.5}Br]^-$ half of the $bcbpy^{2+}$cation resides in the channel, making up most of crystal **1** coordinated with five O atoms from PTA^{4-} and one Br atom. Each PTA^{4-} ligand links with six Cd atoms, as illustrated in Fig. 1b, Cd(1) and Cd(#1), Cd(4) and Cd(#4) are bidentate coordination with six O atoms from four carboxyl of PTA^{4-}, Cd(2) and Cd(3) are monodentate coordination with one O atom from different carboxyl of PTA^{4-}. Meanwhile, we found that the distance between O and N is 3.749 and 3.922 Å, and the distance from Br to the bipyridine ring of $bcbpy^{2-}$ viologen ligand is 3.529 Å displayed in Fig. 1c, they are likely to be pathways of electron transfer and arising the color change of **1** because of the viologen free radical generating [13, 14, 17]. The structure of 1D packing was displayed in Fig. 1d. Crystal data and framework refinements are given in Tables S1, S2 and S3.

Photo- and Thermochromic Behavior

Based on the response of H_2bcbpy·2Br to UV light and blue light, the solid-state UV/visible diffuse reflectivity spectra of H_2bcbpy·2Br ligands (Fig. S5) and crystal samples (Fig. 2) were measured and transformed into absorption spectrum to explore their chromic properties [21–23]. The absorption spectrum of hybrid material **1** shows a strong absorption band in the range of 250 ~ 800 nm, and the absorption of UV light is more potent than that of blue light under the same situation. As shown in Fig. 3, The light-yellow complex sample turns blue since irradiation upon UV light and blue ray. From these results, **1** has better response to UV light compared with the blue light, the decolorized complex could be decolorized after a week in the dark, and the decolorized complex can turn blue again after irradiation, which means that the photochromic behavior of the complex is reversible. The powder XRD profiles and infrared (IR) spectra show no appreciable variations after photochromism (Figs. S6 and S7), suggesting that the crystalline and molecular structures are maintained without bond cleavage or formation, which indicates that the origins of photo- and thermochromic properties for **1** are not photoinduced isomerization or photolysis. To further study the photochrmic mechanism of **1**, electron paramagneticresonance (EPR) spectroscopy and theory study with Guassian 09 were implemented to ensure the involvement of viologen radicals in the chromic progress. As displayed in Fig. S8, the EPR spectroscopy was performed before and after irradiation by UV and blue light, which can explain the production of viologen radicals. Meanwhile, the estimation consequences of molecular frontier orbitals (HOMO and LUMO) also theoretically prove the generation of viologen radicals, which indicated O^{2-} atoms from PTA^{4-} and Br^- as the donor and the N atom as the acceptor of electron (Fig. S9). Compound **1** changes from yellow to green when heated at 90°C for 2 min (Fig. S10), the EPR result exhibited that the production of viologen radicals, which arises the color changing of **1**. From the structure of **1** (Fig. 1a), there was no free and coordination water molecule, so the color changing arises by heat.

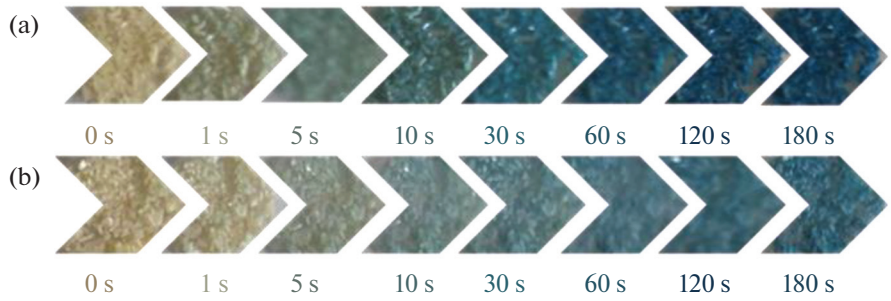

Fig. 3. Graphs of **1** irradiated with (a) UV light and (b) blue rays.

Photoswitchable Luminescence Properties

Considering the luminescence performance of the H_2bcbpy·2Br ligand, the photo-controlled luminescence properties are illustrated in our research as another product of the electron transfer step [18, 19]. Due to the better response to UV light. Compound **1** exhibits evident fluorescence quenching phenomenons under 365 nm UV light irradiation. As displayed in Fig. 4, the fluorescence spectra one demonstrates that when excited at 380 nm, there is a strong emission peak at 500 nm, which may be caused by D–A interactions between the electron donor and bcbpy ligand. In addition, under Uv irradiation, the emission peak decreases rapidly and gradually (365 nm, 40 W). Therefore, the emission intensity is influenced by the ET progress, which results in quenching luminescence. As we see, in Fig. 4, the fluorescent spectrum of hybrid **1** displays a broad, intense absorption band from 410 to about 700 nm, which is like the absorption band of UV/vis diffuse-reflectance spectrum in Fig. 2a.

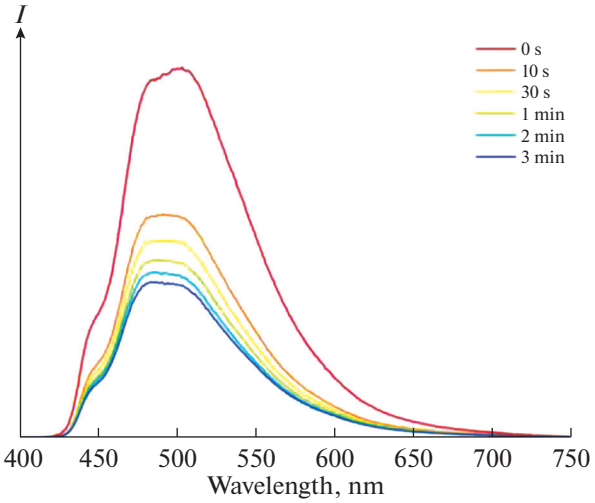

Fig. 4. Luminescence emission spectral changes (λ_{ex} = 380 nm) of **1** after 365 nm UV light irradiation at different time.

The consequences show that photochromism and photo-controlled luminescence could take place at the same time, which is caused by photoinduced electron transfer between the donor (O^{2-} and Br^-) and the acceptor (N^+atom from pyridine of H_2bcbpy·2Br ligand).

Sensing of Organic Ammonia

As we know, viologen ligands (H_2bcbpy·2Br) could be regarded as a kind of Lewis acid (N^+ cations in the pyridine ring). Meanwhile, H_2bcbpy·2Br has good electron-accepting capabilities because of their electron-deficient properties. Meanwhile, ammonia is an excellent electron donor and Lewis's base. Electron rich organic amine molecules can provide electronic properties to CCPs with the viologen moieties within the framework, resulting in a color change. Along these lines, the treatment between **1** and different organic ammonia like, primary ammonia (NH_3, ethylamine and *N*-propylamine and secondary ammonia (diethyamine and dipropylamine) was done. In Fig. 5, when **1** exposures to five different organic ammonia vapors, like most of MOFs and CPs based viologen ligand, exhibits selective adsorption to different organic ammonia. When **1**@NH_3, ethylamine and *N*-propylamine, became light green, dark green and brown separately. However, to secondary ammonia, **1**@diethyamine and dipropylamine amlost have no color change. From Fig. 1d, as we know, the N^+ cation can form interaction with organic ammonia molecules. As follows from the PXRD recorded in situ, the solid saturated with crystalline **1**@ammonia and the positions of lines are very close to the ones of the initial phase **1**, the crystal structure is scarcely not destroyed (Fig. S11). The results illustrated that **1** has better adsorption for primary ammonia molecules based on the basic complex structure and occurs electrostatic adsorption with amine molecules, which have little size and volume, due to the color-changing of **1** in solid state.

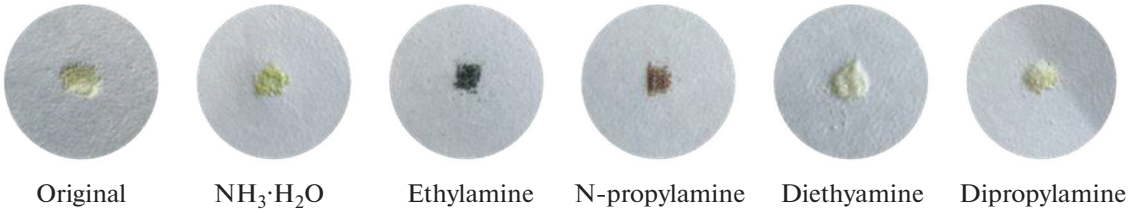

Fig. 5. Graphs of **1** before and after detecting different organic ammonia.

CONCLUSIONS

All in all, in this article, a novel one-dimensional CCP composed of $[Cd(PTA)_{0.5}Br]^-$ and $bcbpy^{2+}$ guest cations has been prepared, named $[Cd(PTA)_{0.5}(bcbpy)_{0.5}Br]$ (**1**). Compound **1** is photoactive and can react with 365 nm UV light and 405 nm blue light rapidly. The photochromic process of **1** formed from the generation of viologen radicals by photo-induced ET progress. Meanwhile, **1** exhibits thermochromism, photo-controlled luminescence and sensing of primary ammonia properties in the solid state.

SUPPLEMENTARY INFORMATION

The online version contains supplementary material available at https://doi.org/10.1134/S0036023624601119.

ACKNOWLEDGMENTS

This project was financially supported by the Natural Science Foundation of Jilin Province (YDZJ202101ZYTS067, YDZJ202101ZYTS072), Education Department Foundation of Jilin Province (JJKH20220045KJ).

FUNDING

This work was supported by ongoing institutional funding. No additional grants to carry out or direct this particular research were obtained.

CONFLICT OF INTEREST

The authors of this work declare that they have no conflicts of interest.

REFERENCES

1. S. E. Korolenko, V. V. Avdeeva, E. A. Malinina, and N. T. Kuznetsov, Russ. J. Inorg. Chem. **66**, 1350 (2021). https://doi.org/10.1134/S0036023621090047
2. V. S. Gusarov, A. M. Cheplakova, D. G. Samsonenko, A. S. Vinogradov, and V. P. Fedin, Russ. J. Inorg. Chem. **66**, 1374 (2021). https://doi.org/10.1134/S0036023621090035
3. Y. Y. Guo, R. D. Wang, W. M. Wei, F. Fang, L. Wang, S. S. Zhang, J. Zhang, L. Du, and Q. H. Zhao, Inorg. Chem. **63**, 3870 (2024). https://doi.org/10.1021/acs.inorgchem.3c04228
4. M. Y. Guo, G. Li, S. L. Yang, R. Bu, X. Q. Piao, and E. Q. Gao, Chem. Eur. J. **27**, 16415 (2021). https://doi.org/10.1002/chem.202102413
5. S. Chand, S. C. Pal, D. W. Lim, K. Otsubo, A. Pal, H. Kitagawa, and M. C. Das, ACS Mater. Lett. **2**, 1343 (2020). https://doi.org/10.1021/acsmaterialslett.0c00358
6. L. Huang, X. N. Li, Y. Shen, R. H. Song, W. B. Cui, and H. Zhang, Dalton Trans. **53**, 5192 (2024). https://doi.org/10.1039/d3dt03647b
7. K. J. Li, Y. Shen, S. L. Li, and X. M. Zhang, Dyes Pigm. **224**, 112033 (2024). https://doi.org/10.1016/j.dyepig.2024.112033
8. W. G. Santos, D. S. Budkina, P. F. G. M. da Costa, D. R. Cardoso, A. N. Tarnovsky, and M. D. E. Forbes, Mater. Adv. **3**, 3862 (2022). https://doi.org/10.1039/d1ma01030a
9. J. Ying, L. Jin, C. X. Sun, A. X. Tian, and X. L. Wang, Chem. Eur. J. **27**, 1 (2021). https://doi.org/10.1002/chem.202103268
10. C. M. Yu, P. H. Wang, Q. Liu, L. Z. Cai, and G. C. Guo, Cryst. Growth Des. **21**, 1323 (2021). https://doi.org/10.1021/acs.cgd.0c01597
11. B. Chen, Y. R. Huang, K. Y. Song, X. L. Lin, H. H. Li, and Z. R. Chen, Chem. Mater. **33**, 2178 (2021). https://doi.org/10.1021/acs.chemmater.1c00090
12. M. Y. Guo, G. Li, S. L. Yang, R. Bu, X. Q. Piao, and E. Q. Gao, Chem. Eur. J. **27**, 16415 (2021). https://doi.org/10.1002/chem.202102413
13. Y. W. Wang, M. H. Li, S. Q. Zhang, X. Fang, and M. J. Lin, Cryst. Eng. Comm. **23**, 6267 (2021). https://doi.org/10.1039/d1ce00789k
14. Z. H. Li, L. P. Xue, Y. Wu, Q. Wang, and B. T. Zhao, Dyes Pigm. **195**, 109743 (2021). https://doi.org/10.1016/j.dyepig.2021.109743
15. G. Zhao, W. Liu, F. Yuan, and J. Liu, Dyes Pigm. **188**, 109196 (2021). https://doi.org/10.1016/j.dyepig.2021.109196
16. L. Liu, Q. Liu, R. Li, M. S. Wang, and G. C. Guo, J. Am. Chem. Soc. **143**, 2232 (2021). https://doi.org/10.1021/jacs.0c10183
17. V. V. Avdeeva, A. S. Kubasov, S. E. Nikiforova, L. V. Goeva, E. A. Malinina, and N. T. Kuznetsov, Russ. J. Inorg. Chem. **68**, 1406 (2023). https://doi.org/10.1134/S0036023623601794

18. X. Yang, C. Yan, Z. Li, X. Li, Q. Yu, T. Sang, Y. Gai, Q. Zhang, and K. Xiong, Inorg. Chem. **60**, 5988 (2021). https://doi.org/10.1021/acs.inorgchem.1c00404
19. J. J. Liu, Z. L. Sun, J. Liu, and S. B. Xia, J. Mol. Struct. **1238**, 130444 (2021). https://doi.org/10.1016/j.molstruc.2021.130444
20. M. Zuo, Y. Liu, N. Yuan, Y. Gao, Y. Li, Y. Ma, M. Sun, and S. Cui, J. Solid State Chem. **307**, 122868 (2022). https://doi.org/10.1016/j.jssc.2021.122868
21. C. Sun, C. Yang, P. X. Li, M. S. Wang, and G. C. Guo, Inorg. Chem. **60**, 9278 (2021). https://doi.org/10.1021/acs.inorgchem.1c01521
22. K. Q. Hu, L. W. Zeng, X. H. Kong, Z. W. Huang, J. P. Yu, L. Mei, Z. F. Chai, and W. Q. Shi, Eur. J. Inorg. Chem. **2021**, 5077 (2021). https://doi.org/10.1002/ejic.202100819
23. G. M. Li, Z. G. Liang, Z. Z. Xue, S. D. Han, J. Pan, and G. M. Wang, Dalton Trans. **51**, 4310 (2022). https://doi.org/10.1039/d2dt00190j